Investigating Permeation Behaviour of Flufenamic Acid Cocrystals Using A Dissolution and Permeation System

Minshan Guo,[†] Ke Wang,[†] Ning Qiao,[‡] Vanessa Yardley,[†§] and Mingzhong Li[†]*

† School of Pharmacy, De Montfort University, Leicester LE1 9BH, UK

‡ College of Materials Science and Engineering, North China University of Science and Technology, Tangshan, 063210, Hebei, China

†§ Department of Infection & Immunity, Faculty of Infectious & Tropical Diseases, London School of Hygiene and Tropical Medicine, Keppel Street, London WC1E 7HT, UK

*Address: School of Pharmacy, De Montfort University, Leicester, LE1 9BH, U.K.

Tel: +44-1162577132; Email: mli@dmu.ac.uk

Table of Contents (TOC)

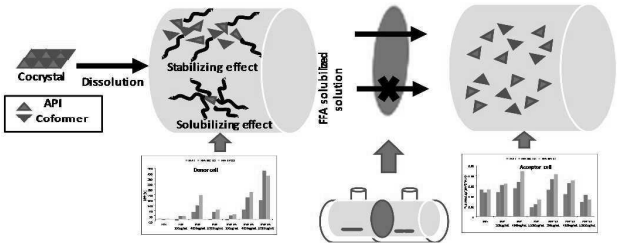

ABSTRACT: The dissolution and permeation of the cocrystals, Flufenamic acid – nicotinamide (FFA-NIC) and Flufenamic acid – theophylline (FFA-TP), have been investigated in the presence of two polymers, polyvinylpyrrolidone (PVP) and copolymer of vinyl pyrrolidone/vinyl acetate (PVP-VA), using a dissolution/permeation (D/P) system. It showed that the types and concentrations of the polymers and their interactions with the coformers had significant effects on the dissolution and permeation of the FFA cocrystals. The role of PVP as a stabilizing agent was not altered in spite of its interaction with the coformer of NIC or TP, which was supported by the proportional flux rate of FFA to the dissolution performance parameter (DPP). With an appropriate PVP concentration, the maximal flux rate of FFA could be obtained for a given FFA cocrystal. The situation was complicated in the presence of PVP-VA. The role of PVP-VA could change due to its association with the coformers, i.e., from a stabilizing agent to a solubilisation agent. In addition, PVP-VA reduced the flux rate of FFA contrasting to its DPP for FFA cocrystals. Finally, ^{1}H NMR provided evidence regarding the molecular interactions between FFA, coformers and polymers at atomic level and gave insight into the mechanism underlying the supersaturated solution and subsequent permeation behaviour of the cocrystals.

KEYWORDS: ***cocrystal, flufenamic acid, ^{1}H NMR, polymer, dissolution, permeation***

1. INTRODUCTION

Over the last decade, pharmaceutical cocrystals have been studied extensively as potential tools to optimise the drug product performance, in particular for compounds with limited aqueous solubility/dissolution rates.[1-3] However, the supersaturated solution generated by dissolution of the highly soluble cocrystals was thermodynamically unstable and the parent drug had a tendency of rapid precipitation.[4-6] It was shown that the parent drug tended to precipitate directly onto the surface of the dissolving cocrystals during dissolution, acting as a coating layer to diminish the dissolution and solubility of the cocrystals.[4, 5] In sight of this, inclusion of effective crystallisation inhibitors in the formulations have been explored to maintain the supersaturated conditions of API (active pharmaceutical ingredient).[4, 6-11] On one occasion, an excess use of coformer or micellar solubilisation decreased the solubility of cocrystals, leading to a lower degree of supersaturation and subsequent prevention of drug precipitation.[7, 8] Maintaining supersaturated drug concentration was also achieved by introducing stabilizing agents in the formulation, that the equilibrium solubility of the drug was not enhanced but the nucleation and/or crystal growth of the drug were inhibited by the intermolecular interactions between the drug molecules and the stabilizing agents. Although polymeric crystallisation inhibitors have been widely used in amorphous solid dispersion formulations to stabilize the amorphous state of the drug substance and to maintain its supersaturated status in solution,[12, 13] such studies have rarely been carried out in cocrystal based formulations.[4, 9, 10, 14-16] The selection of a polymeric excipient in a cocrystal formulation seemed to be much more complicated than those used in the solid dispersion system because the inhibitory ability of the polymers could be undermined significantly by the competitions between the drug, the coformer and the polymer in

terms of hydrogen bondings.[9] Furthermore, a dissolved polymer could alter the dissolution of the cocrystals and subsequently affect its inhibitory ability on the precipitation of the parent drug.[4]

For orally administered solid dosage forms of a drug compound, the elevation of drug concentration in the gastrointestinal (GI) tract did not always improve the absorption as the drug molecules have to permeate across the GI membrane. It was reported that, despite of an increased solubility due to the presence of co-solvent, micelle, cyclodextrin, hydrotropy and emulsifier, a reduced fraction of free drug for membrane permeation by drug encapsulation could eventually lead to very poor drug absorption.[17-25] Therefore, the balance between the solubility and the permeability had to be optimised to achieve the maximal overall absorption of a poorly water soluble drug. The drug permeability of an amorphous solid dispersion formulation was highly polymer dependent.[20, 26-29] A few evidence showed that the cocrystals alone could alter both the solubility and the permeability of the APIs.[30-32] Though it was not clear that, in a cocrystal based formulation, how the permeability of the parent drug was affected by additional polymeric excipients, some speculated that the interplay of the solubility and permeability was the determining factor for a successful formulation.

Our previous investigations found that inclusion of the polymers of polyvinylpyrrolidone (PVP) and copolymer of vinyl pyrrolidone/vinyl acetate (PVP-VA) altered the dissolution of cocrystals of flufenamic acid-nicotinamide (FFA-NIC) and flufenamic acid-theophylline (FFA-TP) and maintained the supersaturation of FFA in solution.[33] In this work we pioneered a systematic examination of key processes occurred during cocrystal dissolution of FFA-NIC and FFA-TP in the absence and presence of PVP or PVP-VA at different concentrations to reveal the kinetics of drug supersaturation and permeation. The molecular structures of FFA

cocrystals and the monomer units of the polymers were shown in Table 1 and a detailed description could be found from previous work.[4, 9, 34, 35] Simultaneous evaluations of the dissolution of FFA cocrystals in the absence and presence of PVP or PVP-VA as well as the permeation of FFA through a dialysis membrane were achieved using a dissolution/permeation (D/P) system (Fig. 1). The dialysis membrane modelled the intestinal epithelium. The D/P system represented a simplified permeation model for quantitative analysis because of the negligible effect of polymer on the membrane.[28, 36, 37] And it had been proved to be a useful tool for examining the absorption of oral drugs after administration.[36-41] In the D/P system, the powdered drug substances were applied to the donor compartment, which was filled with dissolution media in the absence or presence of the polymer at various concentrations, under nonsink conditions to evaluate the ability of the polymer to maintain the supersaturated drug solution. Meanwhile, the amount of FFA molecules permeated into the acceptor compartment, which was filled with the dissolution media, was monitored. The temperature of the whole D/P system was maintained at 37°C using a circulating water bath. The molecular interactions of the FFA, coformers and polymers were analysed by one-dimensional proton nuclear magnetic resonance (^{1}H NMR) spectroscopy. The ^{1}H NMR analysis was conducted in low polarity solvent deuterated chloroform ($CDCl_3$) solutions containing singular, binary and ternary components of FFA, coformers and polymers. The changes of the chemical environment surrounding the molecules would be reflected by the characteristic peak shifts in ^{1}H NMR spectra and the molecular mobility would be reflected by the peak widths.[42-51]

2. MATERIALS AND METHODS

2.1. Materials. Flufenamic acid form I (FFA), Nicotinamide (NIC) (≥99.5% purity), Theophylline (TP) (≥99.5% purity), Potassium dihydrogen phosphate (KH_2PO_4) and sodium hydroxide (NaOH) were purchased from Sigma-Aldrich (Dorset, UK). Plasdone K-29/32 (PVP) and Plasdone S-630 (PVP-VA) were gifts from Ashland Inc. (Schaffhausen, Switzerland). Methanol (HPLC grade) and acetonitrile (HPLC grade) were purchased from Fisher Scientific (Loughborough, UK) and used as received. Double distilled water was generated from a Bi-Distiller (WSC044.MH3.7, Fistreem International Limited, Loughborough, UK) and used throughout the study. Deuterated chloroform ($CDCl_3$) was purchased from Goss Scientific Instruments Ltd (Crewe, UK).

2.2. Methods.

2.2.1. Preparation of 0.01M Phosphate Buffer Solution (PBS), pH 4.5. PBS solution (0.01M, *pH* 4.5) was used as the dissolution medium. It was prepared according to British Pharmacopeia 2010: 1.361g of potassium phosphate monobase was dissolved in double distilled water and the pH of the solution was adjusted to 4.5 using 1 M of sodium hydroxide solution.

2.2.2. Preparation of FFA Cocrystals. As previously described,[9] the cocrystals of FFA-NIC and FFA-TP were prepared with the solvent evaporation and the cooling crystallization methods, respectively. The formation of cocrystals was confirmed by Differential Scanning Colorimetry (DSC), Fourier Transform Infrared Spectroscopy (FTIR) and Powder X-ray Diffraction (PXRD).

2.2.3. The Apparent Equilibrium Solubility Measurement for FFA in the Absence and Presence of Polymers and/or Coformers. To investigate the effect of coformers and/or polymers on the solubility of FFA, 20 mL of 0.01 M PBS (pH 4.5) was used as

the solvent to prepare the solutions of PVP or PVP-VA at concentrations of 200 μg/mL, 500 μg/mL, 1000 μg/mL, 2000 μg/mL, 4000 μg/mL, 8000 μg/mL, 12000 μg/mL and 16000 μg/mL. Appropriate amount of the powdered FFA crystals was then added to these solutions for the apparent equilibrium solubility test. The FFA crystals were slightly grounded by a mortar and pestle and passed through a 60 mesh sieve so that the particle size of the crystals was no more than 250 μm. The test was carried out for 24 h at a temperature of 37 ± 0.5°C with constant mixing at 150 r.p.m. The clear solution was then separated from the remaining solid by centrifugation (MSB 010.CX2.5 centrifuge, MSE Ltd, London, U.K.) at 13,000 r.p.m. for 1 min and the concentration of FFA was determined by High Performance Liquid Chromatography (HPLC).

To investigate the combined effects of coformer and polymer on the solubility of FFA, the above series of PVP or PVP-VA solutions were added with NIC or TP at a concentration of 47.8 μg/mL or 71.1 μg/mL, respectively. The coformer concentration selected in the experiments was based on the flux rate experiments, which 1.43 mg of FFA-NIC and 1.64 mg of FFA-TP were corresponding to 47.8 μg/mL of NIC and 71.1 μg/mL of TP, under the assumption of complete dissolving of the FFA cocrystals. An appropriate amount of the FFA crystals was then added to these solutions for the apparent equilibrium solubility test.

2.2.4. The Dissolution and Permeation Measurements. The D/P system was used to evaluate the dissolution and permeation of cocrystals. It consisted of a donor and an acceptor compartment, which was separated by a regenerated cellulose membrane with a Molecular Weight Cut-Off (MWCO) of 6-8 KDa (Spectrum Labs Inc. Rancho Dominguez, CA 90220, USA) (Fig. 1). Either the donor or acceptor compartment has a capacity of 10 mL. The orifice diameter of the compartment was 0.9 cm,

corresponding to 0.671 cm^2 surface area of the membrane. Like the FFA crystals, the crystalline substance used in this experiment were prepared to sizes that no bigger than 250 μm. 1 mg of single component crystals of FFA or cocrystals with equivalent amount of FFA were firstly added to the donor compartment and this was followed by the addition of 9 mL of 0.01 M PBS (pH 4.5) to the receptor compartment. 9 mL of 0.01 M PBS (pH 4.5) in the absence or presence of PVP or PVP-VA (200 μg/mL, 4000 μg/mL, and 16000 μg/mL) was then added to the donor compartment which contained the crystals. The temperature of the whole system was maintained at 37°C by a circulating water bath. 0.5 mL of the sample was withdrawn from the donor compartment at the time intervals of 5, 10, 15, 30, 60, 120 and 240 mins using a syringe and any volume change due to the withdrawal was immediately compensated with 0.01 M PBS (pH 4.5). The concentrations of FFA were then determined by HPLC.

The dissolution performance parameter (DPP)[52] was used to evaluate the dissolution of the FFA cocrystals, as detailed previously,[4] and the dissolution of FFA crystals was used as the reference. The difference of the DPP of the FFA cocrystals measured in the absence and presence of PVP or PVP-VA would give indication of the effect of the polymers on dissolution and on the maintenance of drug supersaturation.

The flux of a drug through the membrane, which was defined as the amount of drug crossing a unit area perpendicular to its flow direction per unit time t, was calculated using the following equation:

$$J(t) = \frac{(C_{t_2} - C_{t_1})}{A(t_2 - t_1)} V \quad (1)$$

where $J(t)$ was the flux of a drug; C_{t_1} was the drug concentration (μg/mL) at t_1; C_{t_2} was the drug concentration (μg/mL) at t_2; V was the solution volume and A is the area of exposed membrane.

2.2.5. NMR Measurements. ^{1}H NMR was used to identify the interactions between the drug, coformer and polymer in solution. The measurements were carried out with a Bruker AV400 NMR Spectrometer (Bruker UK Limited, Coventry, UK) and the same settings were used throughout the measurements: 64 scans with a relaxation delay of 1 s, a spectral of 8278Hz, a time domain of 32k data and analysing software Mestrenova V11.0 (Mestrelab Research, Escondido, CA 92027, USA).

All the samples were prepared in deuterated chloroform ($CDCl_3$) using the standard 5 mm NMR tubes and the spectra of tetramethysilane (TMS) was used as an internal standard. Detailed measurements were shown in Table S1 in the Supporting Information, which included spectra of the singular component (FFA, NIC, TP, PVP, PVP-VA), the binary components (FFA/NIC, FFA/TP, FFA/PVP, FFA/PVP-VA, NIC/PVP, NIC/PVP-VA, TP/PVP, TP/PVP-VA) and the ternary components (FFA/NIC/PVP, FFA/NIC/PVP-VA, FFA/TP/PVP, FFA/TP/PVP-VA).

To mimic a cocrystal system, the FFA and its coformers were included in the solution at 1:1 molar ratio. Three sets of concentrations were prepared for the simulated cocystal system: 215 μg/mL NIC/ 320 μg/mL TP and 500 μg/mL FFA; 430 μg/mL NIC/640 μg/mL TP and 1000 μg/mL FFA; 2150 μg/mL NIC/3200 μg/mL TP and 5000 μg/mL FFA. For investigation of the effect of polymer on the simulated cocrystal system, PVP or PVP-VA was included in the solution at a concentration of 200 μg/mL or 5000 μg/mL, respectively.

2.2.6. High Performance Liquid Chromatography (HPLC) Analysis. The concentration of FFA, NIC or TP was determined by HEWLETT PACKARD series 1100 automatic HPLC with a Luna@ Omega PS C18 100A LC column (5 μm, 150 × 4.6 mm) (Phenomenex, Inc., Macclesfield, UK). The sample temperature was maintained at 40°C. The conditions used for measurements were listed in Table 2.

3. RESULTS

3.1 Effects of Polymer and/or Coformer on the Equilibrium Solubility of FFA. The effects of polymer and/or coformer on the equilibrium solubility of FFA were shown in Fig. 2. The equilibrium solubility of FFA at 37°C measured in PBS was 9.0 ± 0.7 μg/mL. PVP had a moderate effect, which the solubility of FFA was slightly increased with the PVP concentration of 1000 μg/mL and it reached the maximum of 14.9 ± 1.0 μg/mL at the PVP concentration of 2000 μg/mL. In contrast, the effect of PVP-VA could be seen at the concentration of 1000 μg/mL and it became more prominent with the increase of the concentration. In fact, the solubility of FFA reached 17.2 ± 1.6 μg/mL at a PVP-VA concentration of 4000 μg/mL and 37.6 ± 0.5 μg/mL at a PVP-VA concentration of 16000 μg/mL.

Whereas the presence of NIC seemed to have no effect, the presence of TP at a concentration of 71.1 μg/mL increased the equilibrium solubility of FFA to 10.24 ± 0.71 μg/mL. Neither NIC nor TP altered the equilibrium solubility of FFA in the solution containing PVP. In contrast, the presence of NIC or TP further enhanced the solubility FFA observed in solutions containing PVP-VA.

3.2. Effect of Polymers on the Dissolution and Permeation of FFA Cocrystals. The dialysis membrane acted as a selective barrier for the substances to pass through based on their sizes. The MWCO of the dialysis membrane used in the study was 6-8 KDa and it would thus allow the transfer of FFA, which has a molecular weight (MW) of 281 Da, from the donor compartment

3.2.1. Dissolution and Permeation Performances of FFA, FFA-NIC and FFA-TP in PBS. Fig. 3 (a) showed the dissolution of FFA, FFA-NIC and FFA-TP obtained from the D/P system. It could be seen that FFA-NIC had the fastest dissolution and FFA reached its maximum concentration, 8.8 ± 0.2 μg/mL, within the first 5 min. After

that the FFA concentration measured for FFA-NIC gradually dropped and the minimum concentration, 7.5 ± 0.3 μg/mL, was obtained at 120 min. In contrast, the concentrations measured for FFA and FFA-TP slowly increased to the equilibrium solubility of FFA, 9.0 ± 0.3 μg/mL, at 60 min and remained that concentration afterwards. The quantitative comparison of DPPs[4] were shown in Fig. 4 (a), which FFA-NIC had a lower DDP than that of FFA and FFA-TP.

Fig. 3 (b) showed the permeation of FFA, FFA-NIC and FFA-TP obtained from the D/P system. In the first 60 min, the gradually increased FFA concentrations measured for all three solids overlapped. After that, the concentrations of FFA measured at all three occasions increased steadily and FFA and FFA-TP had a slightly greater rate than that of FFA-NIC. This was in consistent with the mass flux rates shown in Fig. 4 (b).

3.2.2. Effect of PVP or PVP-VA on the Dissolution and Permeation of FFA, FFA-NIC and FFA-TP. Fig. 5 demonstrated the effect of PVP on the dissolution of FFA, FFA-NIC and FFA-TP in the donor compartment and the subsequent permeation of FFA to the acceptor compartment. Both FFA-NIC and FFA-TP showed an enhanced dissolution in comparison to their parent drug FFA when PVP was added to the dissolution media. A supersaturated state of FFA was observed for FFA-TP and FFA-NIC in the dissolution media with PVP at 200 μg/mL, where the concentration of FFA reached 16.7 μg/mL for FFA-TP at 5 min and 12.2 μg/mL for FFA-NIC at 15 min [Fig. 5(a1)]. The concentrations of FFA observed for FFA-NIC and FFA-TP were then gradually reduced to the parent drug's solubility at the 60 min point [Fig. 5(a1)]. Correspondingly, the presence of PVP increased the amount of FFA detected in the acceptor compartment to 1.23-fold for FFA-TP and 1.17-fold for FFA-NIC [Fig. 4 (b)], but decreased the amount of FFA detected at the acceptor compartment by 15.4%

for the parent FFA [Fig. 5 (b1) and Fig. 4 (b)]. All these phenomena suggested that the inclusion of PVP in the dissolution media increased the dissolution and permeation of FFA cocrystals, whereas it slowed down the dissolution as well as the permeation of the parent FFA.

When PVP was added to a concentration of 4000 μg/mL, the concentration of FFA detected in the donor compartment for FFA-TP reached 40 μg/mL at 15 min, which was approximately 4.5-fold of the solubility of FFA [Fig. 5 (a2)]. And the concentration of FFA detected for FFA-NIC at the same time was 23.6 μg/mL. These indicated that FFA-TP had a better dissolution than FFA-NIC. On the other hand, the concentration of FFA detected for FFA-NIC in the donor compartment quickly decreased to 19.5 μg/mL at 15 min and remained constant afterwards. In contrast, the concentration of FFA detected in the donor compartment for FFA-TP decreased slowly from 40 μg/mL and stabilized to 28.8 μg/mL after 60 min. Consequently, the DPP of FFA-TP was 228% higher than that of FFA and was 128% higher that of FFA-NIC [Fig. 4 (a)]. In accordance with these, the amount of FFA detected at the acceptor compartment increased by 1.69-fold in the case of FFA-TP and by 1.27-fold in the case of FFA-NIC [Fig. 5 (b2) and Fig. 4 (b)].

Interestingly, a further increased concentration of PVP to 16000 μg/mL diminished the dissolution of FFA-TP and FFA-NIC, as shown in Figs. 5 (a3) and Fig. 4 (a). The maximal concentration of FFA detected in the donor compartment was 27.5 μg/mL for FFA-TP and 19.7 μg/mL for FFA-NIC. Meanwhile, the amount of FFA permeated cross the membrane reduced significantly for FFA-TP and FFA-NIC [Fig. 5 (b3)]. And the flux rate of the FFA-TP was 0.62-fold of the FFA observed in 0.01 M PBS and 0.45-fold for the FFA-NIC [Fig. 5 (b3) and Fig. 4 (b)]. In addition, in comparison to those measured in PBS, 16000 μg/mL of PVP significantly slowed down the

dissolution of FFA [Fig. 5 (a3)], as demonstrated by a 9% reduction of DPP [Fig. 4 (a)] and a just 0.34-fold of flux rate [Fig. 5 (b3) and Fig. 4 (b)].

The dissolution and permeation measured for FFA and FFA cocrystals in the presence of PVP-VA were shown in Fig. 6. The dissolution of FFA cocrystals was significantly enhanced by PVP-VA. At a PVP-VA concentration of 200 μg/mL, a 33.8% increase of DPP was observed for FFA-NIC and a 42.6% increase of DPP was observed for FFA-TP [Fig. 6 (a1) and Fig. 4 (a)]. At a PVP-VA concentration of 16000 μg/mL, the DPP observed was increased to 460.5% for FFA-NIC and 409.4% for FFA-TP [Fig. 6 (a3) and Fig. 4 (a)]. However, the amount of FFA detected at the acceptor compartment seemed not to be proportional to the corresponding DPPs [Fig. 6 (b3) and Fig. 4 (b)]. Actually, the FFA flux rate of FFA and FFA cocrystals were reduced with the increased concentration of PVP-VA. In spite of that, the FFA flux rates measured for FFA-NIC and FFA-TP at the PVP-VA concentration of 200 μg/mL or 4000 μg/mL were still higher than that measured for FFA in the absence of PVP-VA [Fig. 4 (b)]. Whereas, when the added PVP-VA reached a concentration of 16000 μg/mL the flux rate measured for FFA-NIC or FFA-TP was lower than that measured for FFA in the absence of PVP-VA [Fig. 4 (b)].

3.3. NMR Analysis of Interactions Between FFA, Coformers and Polymers. The ^{1}H NMR experiments were conducted to investigate the interactions between FFA, coformers (NIC and TP) and polymers (PVP and PVP-VA) in solution, and the tests were summarized in Table S1 of the Supplementary Information. Assignments of the ^{1}H chemical shifts of FFA, NIC, TP, PVP and PVP-VA were carried out previously.[49, 53-57] The focus of this work was to examine the characteristic chemical shifts of the protons in each of the molecules of FFA, TP, and NIC. These shifts could be due to the hydrogen bonding or self-aggregation in solution, including i) the

chemical shifts of singlet peak of H_j and two doublet peaks of H_h in FFA; ii) the chemical shifts of H_a, H_b and H_c in NIC; and iii) the chemical shifts of H_a, H_b, H_c and H_d in TP. The detailed information regarding the protons in each molecule could be found in Table 1 and the full ^{1}H NMR spectra of the experiments could be found in Fig. S1 of the Supplementary Information.

3.3.1. ^{1}H NMR Analysis of Single Component of FFA, NIC or TP. Fig. 7 (a) showed the ^{1}H NMR chemical shifts of H_j and H_h in FFA and they seemed to be related to the concentrations of FFA. The existence of the hydrogen bond between the NH_j group and the carbonyl O of the carboxylic acid within FFA had been well illustrated.[54] With an increased concentration, the self-association of FFA could also occur through the inter carboxylic acid hydrogen bondings, which was demonstrated by a downfield chemical shift of H_h from 8.049 ppm at 500 μg/mL to 8.061 ppm at 1000 μg/mL, and to 8.082 ppm at 5000 μg/mL. This could be due to proton deshielding by the hydrogen bonds, which the lengthening of the O-H bond reduced the valence electro density around the proton of H_h. The intermolecular association between the dimer of FFAs did not affect the molecular conformation in solution and the intramolecular N-H_j···O=C was not disrupted.[54] Therefore, at an increased concentration of FFA, the peaks of H_j displayed an upfield shift from 9.463 ppm at 500 μg/mL to 9.443 ppm at 1000 μg/mL, and to 9.410 ppm at 5000 μg/mL. The self-association of NIC in solution occurred through inter-amide hydrogen bonding but not the stacking of the pyridine rings.[58] Therefore, with an increased NIC concentration, the downfield shifts of H_a and H_b were observed. This was in contrast to H_c, whose spectra was almost constant ($\Delta\delta$ = 0.001 at 430 μg/mL and $\Delta\delta$ = 0.005 at 2150 μg/mL) [Fig. 7(b)]. The self-association of TP occurred through the asymmetric dimer involving hydrogen bonding of H_b···O of C-CO-N-CH_d and C=N···H_aN-C.[59] Subsequently, all of the ^{1}H

spectra of H_a and H_b of TP moved to a lower field with an increased concentration, whereas the ^1H chemical shifts of H_c and H_d remained constants ($\Delta\delta$ = 0.003 of H_c and $\Delta\delta$ = 0.005 of H_d at 640 μg/mL and $\Delta\delta$ = 0.013 of H_c and $\Delta\delta$ = 0.020 of H_d at 3200 μg/mL) [Fig. 7(c)].

The ^1H NMR chemical shifts of the polymer PVP or PVP-VA are shown in supporting information in Fig. S1, which were in the range from 4.000 ppm to 1.000 ppm and did not overlap with the peaks of FFA, NIC/TP. Therefore the change of chemical shifts of FFA, NIC/TP in the presence of a polymer was caused by the interaction among molecules.

3.3.2. ^1H NMR Analysis of Binary Components. Samples of FFA, NIC and TP were analysed for ^1H NMR in the presence of PVP or PVP-VA to identify their self-association properties and their interactions with PVP or PVP-VA (Fig. 8). The concentrations used were 1000 μg/mL for FFA, 430 μg/mL for NIC and 640 μg/mL for TP.

In the presence of PVP or PVP-VA at a concentration of 200 μg/mL, the peaks of H_h in FFA had a downfield change, indicating the existence of hydrogen bonding between O-H of the carboxylic acid function group in FFA and the carbonyl O group in PVP or PVP-VA. As O=C of the carboxylic acid function group in FFA did not interact with PVP or PVP-VA, the intramolecular attraction of N-H_j···O=C in FFA was not disrupted. This was indicated by a constant spectra of H_j in FFA in the presence or absence of PVP or PVP-VA [Fig. 8 (a)]. When the concentration of PVP or PVP-VA was increased to 5000 μg/mL, the peaks of H_j and H_h in FFA moved in opposite directions: an upfield (shielding) shift for H_h and a down field shift for H_j. This suggested a different mechanism for the interactions between the FFA and the PVP or PVP-VA polymer. The upfield shift of H_h might associate with the transition

of a solution environment from hydrophilic to hydrophobic as a result of the increased concentration of PVP/PVP-VA, leading to hydrophobic interactions between FFA and PVP/PVP-VA.[57, 60] Obviously, the hydrophobic interaction would affect the conformation of FFA in solution, resulting in change of the intramolecular attraction of N-H_j···O=C and a consequent observation of the downfield shift of H_j. Furthermore, the broader ^{1}H NMR peaks observed for FFA in solution containing PVP was in contrast to those observed in solution containing PVP-VA, indicating that PVP could significantly suppress the mobility of FFA molecules in comparison to PVP-VA.

The peaks of NIC were not affected by PVP or PVP-VA at a concentration of 200 μg/mL [Fig. 8 (b)], implying that there was no or weak interaction between NIC and PVP or PVP-VA. When the concentration of PVP or PVP-VA was increased to 5000 μg/mL, the hydrogen bonding formed between NIC and PVP or PVP-VA was demonstrated as the downfield shifts of ^{1}H NMR peaks of NIC.

^{1}H NMR spectra of TP were complex. It could be affected by the interactions between solute and solvent, solute and solute and solute and polymer. Moreover, dimerization of TP molecules was found to be the dominating factor that affected the ^{1}H chemical shifts of TP in $CDCl_3$.[59] TP was recognised as good proton donor and the dimers of TPs could be disrupted by PVP or PVP-VA in solution. This was proven by the downfield shifts of ^{1}H NMR peaks of TP at a polymer concentration of 200 μg/mL [Fig. 8 (c)]. Interestingly, further increased concentration of the polymers caused an upfield (shielding) shifts of H_b, H_d and H_c in TP.

Within the structure of a solid crystalline FFA-NIC, the hydrogen bonds formed between two FFA and two NIC molecules. In detail, the H_i of amide acid in FFA formed hydrogen bond with the aromatic N of one of the NIC, and the carbonyl O atom of the acid of the same FFA formed another hydrogen bond with the amide H_a or

H_b of the other NIC.[34] It was speculated that, as those formed in solid crystalline, the same interactions might form between FFA and NIC in $CDCl_3$ solution. This was based on the facts of the deshielded chemical shifts of the H_h in FFA and the downfield H_c, H_a and H_b in NIC [Fig. 9 (a)]. As a result of the formation of hydrogen bond between the carbonyl O atom of the acid in FFA and NIC, the intramolecular attraction of N-H_j···O=C was disrupted and the chemical shift of H_j in FFA had a downfield movement.

It was suggested that FFA and TP could form a dimer through the H_i of amide acid in FFA and the aromatic N in TP.[35] This was in consistent with the finding of the significant downfield chemical shift of the H_h in FFA [Fig. 9(b)]. Because the carbonyl O atom of the acid of FFA was not involved in the intermolecular interaction with TP, the intramolecular attraction of N-H_j···O=C of FFA was not disrupted, as shown by the constant spectra of H_j.

3.3.3. ^1H NMR Analysis of Ternary Components. ^{1}H NMR spectra of the mixed samples of FFA, NIC/TP and PVP/PVP-VA were shown in Fig. 10. When the concentration of PVP was set to 200 μg/mL, the characteristic peaks of the H_h and H_j in FFA moved upfield, suggesting that, as a result of the interactions between the FFA and the PVP, the hydrogen bonds formed between the FFA and NIC were disrupted [Fig. 10 (a)]. In contrast, PVP-VA at 200 μg/mL had no effect on the spectra of the H_h and H_j in FFA, indicating that the interaction between the FFA and NIC played a dominant role over the interaction between the FFA and PVP-VA [Fig. 10 (b)]. Increasing PVP or PVP-VA to a concentration of 5000 μg/mL rendered the peaks of H_j and H_h moved to opposite directions [Fig. 10 (a) and Fig. 10-(b)]. This might reflect the dominant effect caused by the hydrophobic interaction between the FFA

and PVP or PVP-VA in comparison to the hydrogen bonds formed between the FFA, NIC and PVP or PVP-VA.

When 200 μg/ml of PVP/PVP-VA was mixed with FFA and TP, the spectra of the H_h in FFA slightly moved upfield while that of the H_j almost had no change. It suggested that the hydrogen bonds formed between the FFA and TP were disturbed by the PVP or PVP-VA [Fig. 10 (c) and Fig. 10 (d)]. At a concentration of 5000 μg/mL, the PVP or PVP-VA rendered the peaks of the H_j and the H_h to opposite directions [Fig. 10 (c) and Fig. 10 (d)]. This was similar to those observed for the mixture of FFA and NIC and, once more, demonstrated the dominating hydrophobic interactions between the FFA and PVP or PVP-VA.

4. DISCUSSION

This research demonstrated that the supersaturated drug concentration generated by the cocrystal dissolution could be maintained through inclusion of a polymeric excipient in the formulation, for example, the supersaturated concentration of FFA generated by dissolution of FFA-NIC or FFA-TP was maintained by PVP or PVP-VA[Fig. 4 (a)].[4, 9, 10] On the other hand, in the presence of PVP or PVP-VA, the DPP detected for FFA-NIC or FFA-TP was proportional to the concentration of the polymers and it was much higher than that detected without PVP or PVP-VA [Fig. 4 (a)]. However, as shown in the D/P system, an elevated concentration of FFA in the donor compartment was not accompanied by an increased flux rate of FFA to the acceptor compartment [Fig, 4 (b)]. This erratic drug permeation could lead to poor drug bioavailability, which was crucially related to the amount of drug molecules that could pass through the GI membrane. Therefore, it was important to explore the interplay of the solubility and permeability in the cocrystal based formulation, that enhanced solubility/dissolution might have positive, negative or no effect on the

subsequent permeability.[18-20, 29] The mechanism of how a polymer affected the dissolution of the cocrystals had been investigated, and it seemed that the polymer could interact with the surface of the cocrystal to alter both the dissolution and precipitation.[4] As a further investigation, this research revealed the interactions between the drug substance (FFA), the coformer (NIC or TP) and the polymer (PVP or PVP-VA) in solution and how these interactions maintain the supersaturated drug concentration and the subsequent permeation of the drug substance.

Both PVP and PVP-VA are water soluble polymers. However, due to their structural difference (Table 1), the intermolecular interactions between PVP/PVP-VA and the drug substance FFA or coformer (NIC or TP) were different. This could affect not only the nucleation and growth kinetics[9] but also the permeation of FFA in solution [Fig. 4 (b)]. Interestingly, at the same concentration, PVP-VA always rendered a higher DPP for FFA-NIC and FFA-TP than PVP [Fig. 4(a)]. In contrary, the effect of PVP-VA on the flux rate of FFA-NIC or FFA-TP could be greater or smaller than PVP, which was seemingly concentration dependent (Fig. 4). In fact, for FFA-NIC and FFA-TP, while the FFA flux rates and DPPs measured were in proportion to the concentration of PVP, the FFA flux rates measured were in contrast to the DPPs in the presence of PVP-VA (Fig. 4). Therefore, it was essential to take into account both the flux rate and DPP when evaluating a cocrystal based formulation.

Based on the results in Fig.2, PVP could act as a stabilizing agent in the formulation as the equilibrium solubility of FFA was not increased significantly across the whole range of the concentrations of PVP. The hydrogen bonds between FFA and PVP should be the dominant force when the concentration of PVP was below 4000 μg/mL, which was confirmed by the downfield chemical shifts of H_h in FFA [Fig. 8 (a)]. The

flux rate was determined by the degree of supersaturation (ratio of dissolved amount of unchanged API to its thermodynamic solubility), which was the driving force for transporting the drug substance across the membrane.[29] PVP might inhibit the nucleation of FFA to maintain its supersaturated concentration [Fig. 5 (a)][9] and to increase the flux rate of FFA across the regenerated cellulose membrane [Fig.5 (b)].[29] Due to the bulk precipitation dissolution mechanism, the higher supersaturation concentration of FFA generated by FFA-TP led to a higher flux rate in comparison to FFA-NIC.[4]

When the concentration of PVP was above 4000 μg/mL, the attraction between FFA and PVP changed into hydrophobic interaction due to the confined spaces between the FFA and PVP molecules. This was confirmed by the upfield chemical shifts of H_h in FFA [Fig. 8 (a)]. It must be stressed that, at such a concentration, micellization of PVP did not occur due to its rigorous backbone structure and, therefore, PVP had no significant effect on the equilibrium solubility of FFA (Fig. 2). Consequently, the mobility of FFA in solution was seen to reduce with the increased concentration of PVP, as illustrated by the broaden peak of the H_j in FFA [Fig. 8 (a)].

The reduced flux rate of FFA at a PVP concentration of 16000 μg/mL [Fig. 4 (b)] was the result of a combined effects of the reduced dissolution of the cocrystals [Fig. 5 (a)] and the reduced solute activity coefficient.[37] Although the interaction between FFA and PVP was disturbed by the interaction between PVP and the coformers (Fig. 9 and Fig. 10), the role of PVP as a stabilizing agent did not change, as demonstrated by the minor change of FFA solubility with or without the presence of the coformers (Fig. 2). As a consequence, the flux rate of FFA solely depended on the DPP of the cocrystals, which the maximal flux rate of FFA was observed for FFA-TP in the presence of 4000 μg/mL of PVP.

As seen in Fig.2, PVP-VA had a transitional role in the cocrystal formulation, depending on its concentrations. At a concentration of up to 1000 μg/mL and the absence of NIC or TP, PVP-VA acted as a stabilizing agent as it had no effect on the equilibrium solubility of FFA (Fig. 2). The downfield shifts of the H_h in FFA indicated the formation of hydrogen bond between the FFA and the PVP-VA [Fig. 8 (a)]. Compared to PVP, PVP-VA was more hydrophobic and flexible, leading to micellization at a higher concentration.[61] This research set the critical micelle concentration (CMC) of PVP-VA at 4000 μg/mL. Therefore, at a concentration over the CMC, PVP-VA significantly increased the solubility of FFA. The ^{1}H NMR spectra of FFA showed the upfield shifts of the H_h at PVP-VA concentration of 5000 μg/mL [Fig. 8 (a)], from which the conclusion could be drawn that the encapsulation of FFA took place in PVP-VA micelles. In other words, the role of PVP-VA changed to a solubilisation agent in the formulation.

In the presence of NIC or TP, PVP-VA demonstrated a significant solubilisation capacity (Fig. 2). It was likely that the association of PVP-VA with a coformer , as shown in Fig. 8 (b) and Fig. 8(c), provided an expanded region of the inner core for drug solubilization.[62] The CMC of PVP-VA reduced significantly around 200 μg/mL, at which point the equilibrium solubility of FFA started to increase (Fig. 2). Taken together, it seemed that PVP-VA behaved as a solubilisation agent in the cocrystal formulations regardless of its concentrations.

Corresponding to the increased equilibrium solubility of FFA, the DPPs of the FFA cocrystals were proportional to the concentration of PVP-VA [Fig. 4 (a)]. From the perspective of thermodynamics, an elevated drug concentration due to the presence of PVP-VA was fundamentally different from the drug supersaturation generated by the stabilizing agent of PVP. Solubilizing agent, such as PVP-VA, affected the

concentrations by increasing the equilibrium solubility rather than increasing the chemical potential (degree of supersaturation), as shown by the reduced flux rate of FFA across the membrane [Fig. 4 (b)]. This was in consistent with the findings from previous studies.[18-20, 29]

Overall, the permeation of a FFA cocrystal could be affected by a series of factors, such as the types of polymers, the concentrations of the polymers and coformers. In particular, the interactions between the polymer and the coformer might play roles in improving the absorption of the drug substance.

5. CONCLUSION

The dissolution and permeation of the cocrystals, FFA-NIC and FFA-TP, in the presence of polymers, PVP and PVP-VA, were examined using a dissolution/permeation (D/P) system. It showed that the types of polymers, their concentrations and interactions with coformers were the determining factors. The role of PVP as a stabilizing agent was not altered in spite of its interactions with the coformers of NIC and TP, which was supported by the fact that the flux rate of FFA solely depended on the DPP of the cocrystals. With an appropriate PVP concentration, the maximal flux rate of FFA could be obtained for a given FFA cocrystal. The role of PVP-VA could change due to its association with the coformers, such as from a stabilizing agent to a solubilisation agent. It was also found that PVP-VA rendered the measurement of flux rate contrasting to the measurement of the corresponding DPP. The maximal flux rate of FFA could only be obtained at a very low concentration of PVP-VA. At last, ^{1}H NMR provided evidence regarding the molecular interactions between the FFA, the coformers and the polymers at the atomic level. In conclusion, understanding the relationships between the drug substance, coformers and polymers

at molecular level was the key to optimise the solubility and permeability to maximize the performance of cocrystal based oral drug products.

ASSOCIATED CONTENT

Supporting Information

1) **Table S1.** List of ^{1}H NMR samples.

2) **Figure S1.** All ^{1}H NMR results.

AUTHOR INFORMATION

Corresponding Author

*E-mail: mli@dmu.ac.uk; Tel: +44-1162577132.

Notes

The authors declare no competing financial interest.

ACKNOWLEDGEMENTS

We would like to thank the financial support of the work by UK Engineering and Physical Sciences Research Council (EPSRC, EP/R021198/1) and Science and Technology Project of Hebei Province of China (NO. 16211505). De Montfort University and the Great Britain-China Educational Trust are gratefully acknowledged for providing scholarships for Miss Minshan Guo to conduct her PhD study. We also thank Dr. Ketan Ruparelia at De Montfort University for his help in ^{1}H NMR experiments.

REFERENCES

1. Duggirala, N. K.; Perry, M. L.; Almarsson, O.; Zaworotko, M. J., Pharmaceutical cocrystals: along the path to improved medicines. *Chem. Commun. (Camb.)* **2016,** *52*, 640-55.
2. Kuminek, G.; Cao, F.; da Rocha, A. B. d. O.; Cardoso, S. G.; Rodríguez-Hornedo, N., Cocrystals to facilitate delivery of poorly soluble compounds beyond-rule-of-5. *Adv. Drug. Deliv. Rev.* **2016,** *101*, 143-166.
3. Qiao, N.; Li, M.; Schlindwein, W.; Malek, N.; Davies, A.; Trappitt, G., Pharmaceutical cocrystals: an overview. *Int. J. Pharm.* **2011,** *419*, 1-11.
4. Guo, M.; Wang, K.; Qiao, N.; Fábián, L.; Sadiq, G.; Li, M., Insight into Flufenamic Acid Cocrystal Dissolution in the Presence of a Polymer in Solution: from Single Crystal to Powder Dissolution. *Molecular Pharmaceutics* **2017,** *14*, 4583-4596.
5. Qiao, N.; Wang, K.; Schlindwein, W.; Davies, A.; Li, M., In situ monitoring of carbamazepine–nicotinamide cocrystal intrinsic dissolution behaviour. *European Journal of Pharmaceutics and Biopharmaceutics* **2013,** *83*, 415-426.
6. Remenar, J. F.; Peterson, M. L.; Stephens, P. W.; Zhang, Z.; Zimenkov, Y.; Hickey, M. B., Celecoxib:Nicotinamide Dissociation: Using Excipients To Capture the Cocrystal's Potential. *Molecular Pharmaceutics* **2007,** *4*, 386-400.
7. Yamashita, H.; Sun, C. C., Harvesting Potential Dissolution Advantages of Soluble Cocrystals by Depressing Precipitation Using the Common Coformer Effect. *Crystal Growth & Design* **2016,** *16*, 6719-6721.
8. Cao, F.; Amidon, G. L.; Rodriguez-Hornedo, N.; Amidon, G. E., Mechanistic Analysis of Cocrystal Dissolution as a Function of pH and Micellar Solubilization. *Molecular Pharmaceutics* **2016,** *13*, 1030-1046.
9. Guo, M.; Wang, K.; Hamill, N.; Lorimer, K.; Li, M., Investigating the Influence of Polymers on Supersaturated Flufenamic Acid Cocrystal Solutions. *Molecular Pharmaceutics* **2016,** *13*, 3292-3307.
10. Qiu, S.; Lai, J.; Guo, M.; Wang, K.; Lai, X.; Desai, U.; Juma, N.; Li, M., Role of polymers in solution and tablet-based carbamazepine cocrystal formulations. *CrystEngComm* **2016,** *18*, 2664-2678.
11. Li, M.; Qiu, S.; Lu, Y.; Wang, K.; Lai, X.; Rehan, M., Investigation of the Effect of Hydroxypropyl Methylcellulose on the Phase Transformation and Release Profiles of Carbamazepine-Nicotinamide Cocrystal. *Pharm Res* **2014,** *31*, 2312-2325.
12. Crowley, K. J.; Zografi, G., The Effect of Low Concentrations of Molecularly Dispersed Poly(Vinylpyrrolidone) on Indomethacin Crystallization from the Amorphous State. *Pharm Res* **2003,** *20*, 1417-1422.
13. DiNunzio, J. C.; Miller, D. A.; Yang, W.; McGinity, J. W.; Williams, R. O., Amorphous Compositions Using Concentration Enhancing Polymers for Improved Bioavailability of Itraconazole. *Mol. Pharm.* **2008,** *5*, 968-980.
14. Ullah, M.; Raza Shah, M.; Asad, H. B.; Hassham, M.; Farid Hasan, S.; Hussain, I., Improved in vitro and in vivo performance of carbamazepine enabled by using a succinic acid cocrystal in a stable suspension formulation. *Pak. J. Pharm. Sci.* **2017,** *30*.
15. Ullah, M.; Ullah, H.; Murtaza, G.; Mahmood, Q.; Hussain, I., Evaluation of influence of various polymers on dissolution and phase behavior of carbamazepine-succinic acid cocrystal in matrix tablets. *BioMed research international* **2015,** *2015*.
16. Ullah, M.; Hussain, I.; Sun, C. C., The development of carbamazepine-succinic acid cocrystal tablet formulations with improved in vitro and in vivo performance. *Drug Dev. Ind. Pharm.* **2016,** *42*, 969-976.
17. Beig, A.; Lindley, D.; Miller, J. M.; Agbaria, R.; Dahan, A., Hydrotropic Solubilization of Lipophilic Drugs for Oral Delivery: The Effects of Urea and Nicotinamide on Carbamazepine Solubility–Permeability Interplay. *Frontiers in Pharmacology* **2016,** *7*, 379.

18. Dahan, A.; Beig, A.; Lindley, D.; Miller, J. M., The solubility–permeability interplay and oral drug formulation design: Two heads are better than one. *Advanced Drug Delivery Reviews* **2016,** *101*, 99-107.
19. Dahan, A.; Miller, J. M., The Solubility–Permeability Interplay and Its Implications in Formulation Design and Development for Poorly Soluble Drugs. *The AAPS Journal* **2012,** *14*, 244-251.
20. Beig, A.; Miller, J. M.; Lindley, D.; Carr, R. A.; Zocharski, P.; Agbaria, R.; Dahan, A., Head-To-Head Comparison of Different Solubility-Enabling Formulations of Etoposide and Their Consequent Solubility–Permeability Interplay. *Journal of Pharmaceutical Sciences* **2015,** *104*, 2941-2947.
21. Miller, J. M.; Beig, A.; Carr, R. A.; Webster, G. K.; Dahan, A., The solubility-permeability interplay when using cosolvents for solubilization: revising the way we use solubility-enabling formulations. *Mol. Pharm.* **2012,** *9*, 581-90.
22. Beig, A.; Miller, J. M.; Dahan, A., Accounting for the solubility–permeability interplay in oral formulation development for poor water solubility drugs: The effect of PEG-400 on carbamazepine absorption. *European Journal of Pharmaceutics and Biopharmaceutics* **2012,** *81*, 386-391.
23. Beig, A.; Miller, J. M.; Lindley, D.; Dahan, A., Striking the Optimal Solubility–Permeability Balance in Oral Formulation Development for Lipophilic Drugs: Maximizing Carbamazepine Blood Levels. *Molecular Pharmaceutics* **2017,** *14*, 319-327.
24. Fine-Shamir, N.; Beig, A.; Zur, M.; Lindley, D.; Miller, J. M.; Dahan, A., Toward Successful Cyclodextrin Based Solubility-Enabling Formulations for Oral Delivery of Lipophilic Drugs: Solubility–Permeability Trade-Off, Biorelevant Dissolution, and the Unstirred Water Layer. *Molecular Pharmaceutics* **2017,** *14*, 2138-2146.
25. Miller, J. M.; Beig, A.; Carr, R. A.; Spence, J. K.; Dahan, A., A Win–Win Solution in Oral Delivery of Lipophilic Drugs: Supersaturation via Amorphous Solid Dispersions Increases Apparent Solubility without Sacrifice of Intestinal Membrane Permeability. *Molecular Pharmaceutics* **2012,** *9*, 2009-2016.
26. Frank, K. J.; Rosenblatt, K. M.; Westedt, U.; Hölig, P.; Rosenberg, J.; Mägerlein, M.; Fricker, G.; Brandl, M., Amorphous solid dispersion enhances permeation of poorly soluble ABT-102: True supersaturation vs. apparent solubility enhancement. *International Journal of Pharmaceutics* **2012,** *437*, 288-293.
27. Frank, K. J.; Westedt, U.; Rosenblatt, K. M.; Hölig, P.; Rosenberg, J.; Mägerlein, M.; Fricker, G.; Brandl, M., What Is the Mechanism Behind Increased Permeation Rate of a Poorly Soluble Drug from Aqueous Dispersions of an Amorphous Solid Dispersion? *Journal of Pharmaceutical Sciences* **2014,** *103*, 1779-1786.
28. Beig, A.; Fine-Shamir, N.; Lindley, D.; Miller, J. M.; Dahan, A., Advantageous Solubility-Permeability Interplay When Using Amorphous Solid Dispersion (ASD) Formulation for the BCS Class IV P-gp Substrate Rifaximin: Simultaneous Increase of Both the Solubility and the Permeability. *The AAPS Journal* **2017,** *19*, 806-813.
29. Borbás, E.; Sinkó, B. l.; Tsinman, O.; Tsinman, K.; Kiserdei, E. v.; Démuth, B. z.; Balogh, A.; Bodák, B.; Domokos, A. s.; Dargó, G., Investigation and mathematical description of the real driving force of passive transport of drug molecules from supersaturated solutions. *Mol. Pharm.* **2016,** *13*, 3816-3826.
30. Sanphui, P.; Devi, V. K.; Clara, D.; Malviya, N.; Ganguly, S.; Desiraju, G. R., Cocrystals of Hydrochlorothiazide: Solubility and Diffusion/Permeability Enhancements through Drug–Coformer Interactions. *Molecular Pharmaceutics* **2015,** *12*, 1615-1622.
31. Yan, Y.; Chen, J.-M.; Lu, T.-B., Simultaneously enhancing the solubility and permeability of acyclovir by crystal engineering approach. *CrystEngComm* **2013,** *15*, 6457-6460.

32. Ferretti, V.; Dalpiaz, A.; Bertolasi, V.; Ferraro, L.; Beggiato, S.; Spizzo, F.; Spisni, E.; Pavan, B., Indomethacin Co-Crystals and Their Parent Mixtures: Does the Intestinal Barrier Recognize Them Differently? *Molecular Pharmaceutics* **2015,** *12*, 1501-1511.
33. Guo, M.; Wang, K.; Qiao, N.; Fábián, L.; Sadiq, G.; Li, M., Insight into Flufenamic Acid Cocrystal Dissolution in the Presence of a Polymer in Solution: from Single Crystal to Powder Dissolution. *Molecular Pharmaceutics* **2017**.
34. Fábián, L.; Hamill, N.; Eccles, K. S.; Moynihan, H. A.; Maguire, A. R.; McCausland, L.; Lawrence, S. E., Cocrystals of Fenamic Acids with Nicotinamide. *Crystal Growth & Design* **2011,** *11*, 3522-3528.
35. Aitipamula, S.; Wong, A. B. H.; Chow, P. S.; Tan, R. B. H., Cocrystallization with flufenamic acid: comparison of physicochemical properties of two pharmaceutical cocrystals. *CrystEngComm* **2014,** *16*, 5793-5801.
36. Raina, S. A.; Zhang, G. G. Z.; Alonzo, D. E.; Wu, J.; Zhu, D.; Catron, N. D.; Gao, Y.; Taylor, L. S., Enhancements and Limits in Drug Membrane Transport Using Supersaturated Solutions of Poorly Water Soluble Drugs. *Journal of Pharmaceutical Sciences* **2014,** *103*, 2736-2748.
37. Raina, S. A.; Zhang, G. G. Z.; Alonzo, D. E.; Wu, J.; Zhu, D.; Catron, N. D.; Gao, Y.; Taylor, L. S., Impact of Solubilizing Additives on Supersaturation and Membrane Transport of Drugs. *Pharm Res* **2015,** *32*, 3350-3364.
38. Kataoka, M.; Masaoka, Y.; Yamazaki, Y.; Sakane, T.; Sezaki, H.; Yamashita, S., In Vitro System to Evaluate Oral Absorption of Poorly Water-Soluble Drugs: Simultaneous Analysis on Dissolution and Permeation of Drugs. *Pharm Res* **2003,** *20*, 1674-1680.
39. Kataoka, M.; Masaoka, Y.; Sakuma, S.; Yamashita, S., Effect of Food Intake on the Oral Absorption of Poorly Water-Soluble Drugs: In Vitro Assessment of Drug Dissolution and Permeation Assay System. *Journal of Pharmaceutical Sciences* **2006,** *95*, 2051-2061.
40. Buch, P.; Langguth, P.; Kataoka, M.; Yamashita, S., IVIVC in oral absorption for fenofibrate immediate release tablets using a dissolution/permeation system. *Journal of Pharmaceutical Sciences* **2009,** *98*, 2001-2009.
41. Kataoka, M.; Sugano, K.; da Costa Mathews, C.; Wong, J. W.; Jones, K. L.; Masaoka, Y.; Sakuma, S.; Yamashita, S., Application of Dissolution/Permeation System for Evaluation of Formulation Effect on Oral Absorption of Poorly Water-Soluble Drugs in Drug Development. *Pharm. Res.* **2012,** *29*, 1485-1494.
42. Abu-Diak, O. A.; Jones, D. S.; Andrews, G. P., An Investigation into the Dissolution Properties of Celecoxib Melt Extrudates: Understanding the Role of Polymer Type and Concentration in Stabilizing Supersaturated Drug Concentrations. *Molecular Pharmaceutics* **2011,** *8*, 1362-1371.
43. Maniruzzaman, M.; Morgan, D. J.; Mendham, A. P.; Pang, J.; Snowden, M. J.; Douroumis, D., Drug–polymer intermolecular interactions in hot-melt extruded solid dispersions. *International Journal of Pharmaceutics* **2013,** *443*, 199-208.
44. Ueda, K.; Higashi, K.; Limwikrant, W.; Sekine, S.; Horie, T.; Yamamoto, K.; Moribe, K., Mechanistic Differences in Permeation Behavior of Supersaturated and Solubilized Solutions of Carbamazepine Revealed by Nuclear Magnetic Resonance Measurements. *Molecular Pharmaceutics* **2012,** *9*, 3023-3033.
45. Ueda, K.; Higashi, K.; Yamamoto, K.; Moribe, K., Inhibitory Effect of Hydroxypropyl Methylcellulose Acetate Succinate on Drug Recrystallization from a Supersaturated Solution Assessed Using Nuclear Magnetic Resonance Measurements. *Molecular Pharmaceutics* **2013,** *10*, 3801-3811.
46. Ueda, K.; Higashi, K.; Yamamoto, K.; Moribe, K., Equilibrium State at Supersaturated Drug Concentration Achieved by Hydroxypropyl Methylcellulose Acetate Succinate: Molecular Characterization Using 1H NMR Technique. *Molecular Pharmaceutics* **2015,** *12*, 1096-1104.

47. Ueda, K.; Higashi, K.; Moribe, K., Direct NMR Monitoring of Phase Separation Behavior of Highly Supersaturated Nifedipine Solution Stabilized with Hypromellose Derivatives. *Molecular Pharmaceutics* **2017,** *14*, 2314-2322.
48. Ueda, K.; Higashi, K.; Yamamoto, K.; Moribe, K., In situ molecular elucidation of drug supersaturation achieved by nano-sizing and amorphization of poorly water-soluble drug. *European Journal of Pharmaceutical Sciences* **2015,** *77*, 79-89.
49. Roscigno, P.; Asaro, F.; Pellizer, G.; Ortona, O.; Paduano, L., Complex Formation between Poly(vinylpyrrolidone) and Sodium Decyl Sulfate Studied through NMR. *Langmuir* **2003,** *19*, 9638-9644.
50. Prasad, D.; Chauhan, H.; Atef, E., Role of Molecular Interactions for Synergistic Precipitation Inhibition of Poorly Soluble Drug in Supersaturated Drug–Polymer–Polymer Ternary Solution. *Molecular Pharmaceutics* **2016,** *13*, 756-765.
51. Chen, Y.; Wang, S.; Wang, S.; Liu, C.; Su, C.; Hageman, M.; Hussain, M.; Haskell, R.; Stefanski, K.; Qian, F., Sodium Lauryl Sulfate Competitively Interacts with HPMC-AS and Consequently Reduces Oral Bioavailability of Posaconazole/HPMC-AS Amorphous Solid Dispersion. *Molecular Pharmaceutics* **2016,** *13*, 2787-2795.
52. Chen, Y.; Liu, C.; Chen, Z.; Su, C.; Hageman, M.; Hussain, M.; Haskell, R.; Stefanski, K.; Qian, F., Drug–Polymer–Water Interaction and Its Implication for the Dissolution Performance of Amorphous Solid Dispersions. *Molecular Pharmaceutics* **2015,** *12*, 576-589.
53. Singha, N. C.; Sathyanarayana, D. N., 1H and 13C NMR spectral studies of conformation of some N-(2-pyridinyl)-3-pyridinecarboxamides. *Journal of Molecular Structure* **1998,** *449*, 91-98.
54. Munro, S. L. A.; Craik, D. J., NMR conformational studies of fenamate non-steroidal anti-inflammatory drugs. *Magnetic Resonance in Chemistry* **1994,** *32*, 335-342.
55. You, Z. Y.; Chen, Y. J.; Wang, Y. Y.; Chen, C., Synthesis of Deuterium Labeled Standards of 1-Benzylpiperazine, Fenetylline, Nicocodeine and Nicomorphine. *Journal of the Chinese Chemical Society* **2008,** *55*, 663-667.
56. Ma, J.-h.; Guo, C.; Tang, Y.-l.; Zhang, H.; Liu, H.-z., Probing Paeonol−Pluronic Polymer Interactions by 1H NMR Spectroscopy. *The Journal of Physical Chemistry B* **2007,** *111*, 13371-13378.
57. Ma, J.-h.; Guo, C.; Tang, Y.-l.; Chen, L.; Bahadur, P.; Liu, H.-z., Interaction of Urea with Pluronic Block Copolymers by 1H NMR Spectroscopy. *The Journal of Physical Chemistry B* **2007,** *111*, 5155-5161.
58. Charman, W.; Lai, C.; Craik, D.; Finnin, B.; Reed, B., Self-Association of Nicotinamide in Aqueous-Solution: N.M.R. Studies of Nicotinamide and the Mono- and Di-methyl-Substituted Amide Analogs. *Australian Journal of Chemistry* **1993,** *46*, 377-385.
59. Bobrovs, R.; Seton, L.; Dempster, N., The reluctant polymorph: investigation into the effect of self-association on the solvent mediated phase transformation and nucleation of theophylline. *CrystEngComm* **2015,** *17*, 5237-5251.
60. Otsuka, N.; Ueda, K.; Ohyagi, N.; Shimizu, K.; Katakawa, K.; Kumamoto, T.; Higashi, K.; Yamamoto, K.; Moribe, K., An Insight into Different Stabilization Mechanisms of Phenytoin Derivatives Supersaturation by HPMC and PVP. *Journal of Pharmaceutical Sciences* **2015,** *104*, 2574-2582.
61. Humpolíčková, J.; Štěpánek, M.; Procházka, K.; Hof, M., Solvent Relaxation Study of pH-Dependent Hydration of Poly(oxyethylene) Shells in Polystyrene-block-poly(2-vinylpyridine)-block-poly(oxyethylene) Micelles in Aqueous Solutions. *The Journal of Physical Chemistry A* **2005,** *109*, 10803-10812.
62. Oliveira, C. P.; Ribeiro, M. E.; Ricardo, N. M.; Souza, T. V.; Moura, C. L.; Chaibundit, C.; Yeates, S. G.; Nixon, K.; Attwood, D., The effect of water-soluble polymers, PEG and PVP, on the solubilisation of griseofulvin in aqueous micellar solutions of Pluronic F127. *Int. J. Pharm.* **2011,** *421*, 252-7.

Table 1. Molecular structures of FFA, coformers (NIC and TP), FFA cocrystals (FFA-NIC and FFA-TP) and polymers (PVP and PVP-VA).

FFA	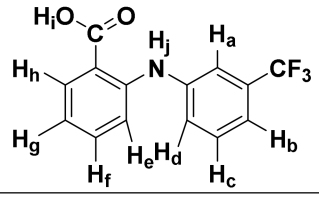
NIC	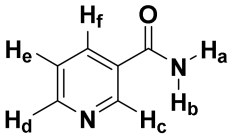
TP	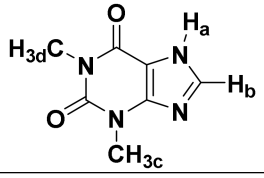
FFA-NIC	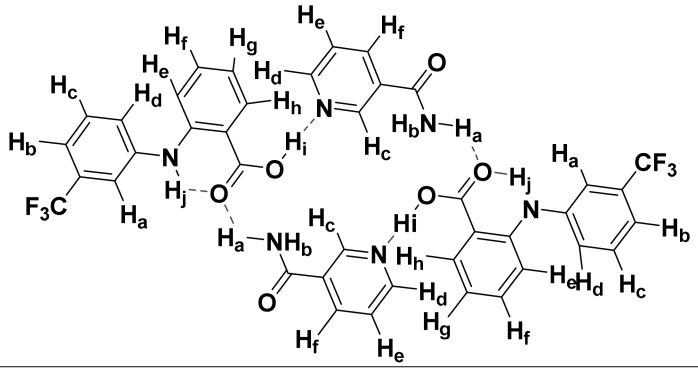
FFA-TP	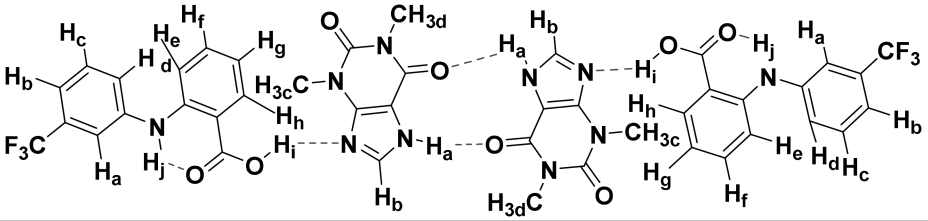
PVP	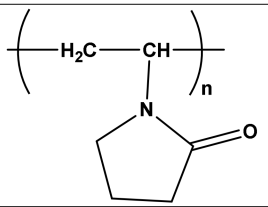
PVP-VA	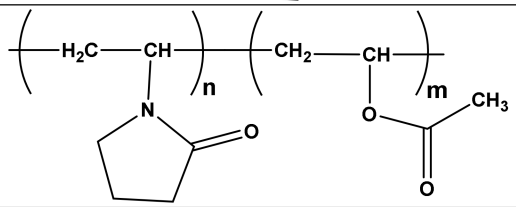

Table 2. HPLC methods

	Mobile phase	Flow rate (mL/min)	Detection wavelength (nm)
FFA	14.5% water (with 0.5% formic acid), 85% methanol	1.5	286
NIC	10% methanol, 90% water	1	265
TP	40% methanol, 60% water	1	265

Figure 1. Diagram of the dissolution/permeation (D/P) system.

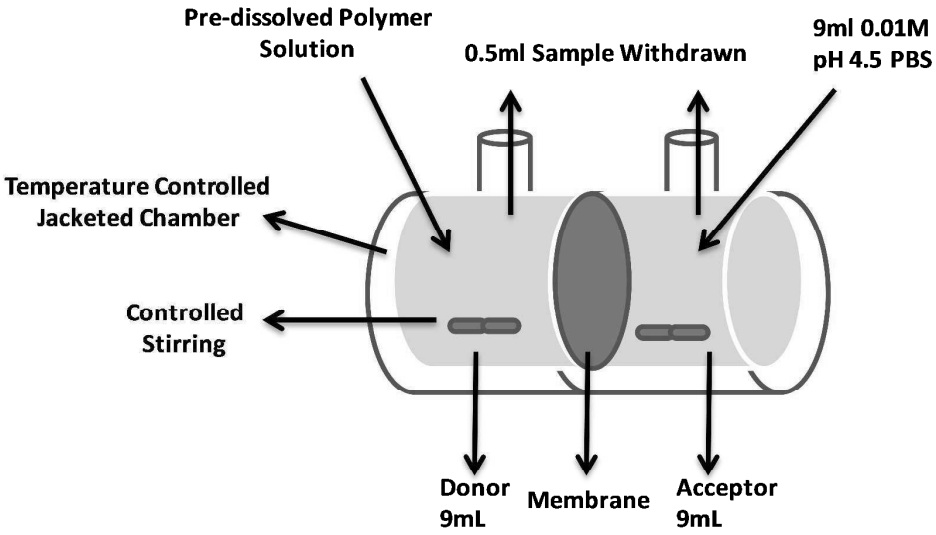

Figure 2. Effect of polymer and/or conformer on the equilibrium solubility of FFA. The apparent equilibrium solubility of FFA were measured in 0.01 M PBS (pH 4.5) with or without PVP or PVP-VA. The concentrations of NIC or TP used were 47.8 μg/mL and 71.1 μg/mL.

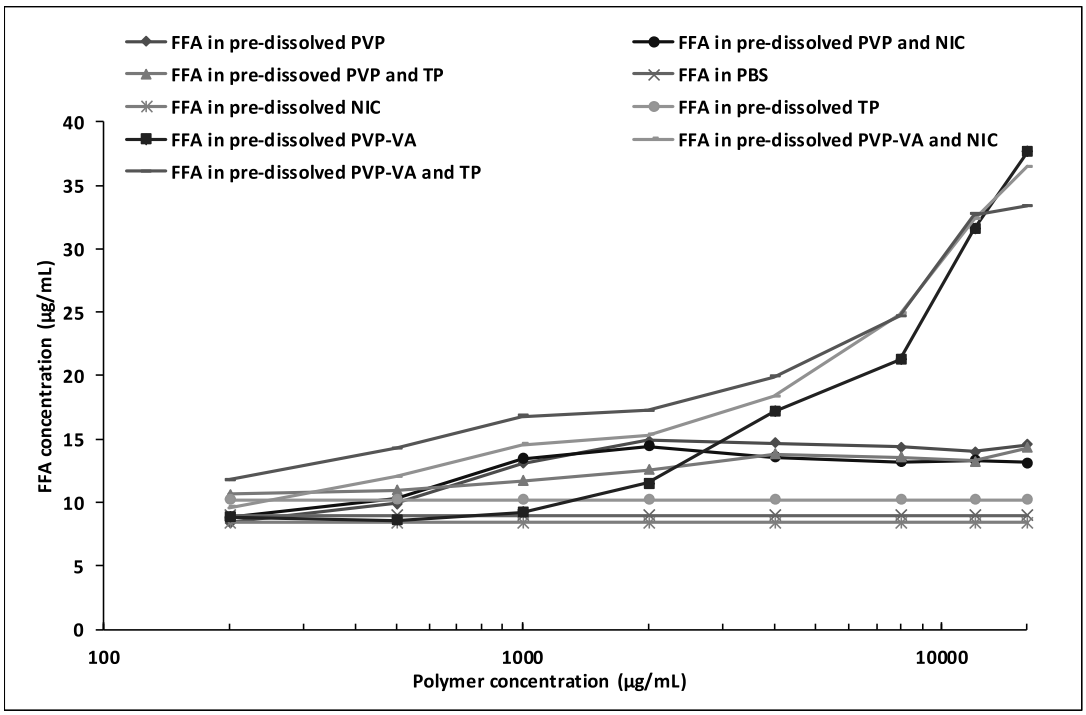

Figure 3. The dissolution (a) and permeation (b) of the FFA, FFA-NIC and FFA-TP were measured using the dissolution/permeation (D/P) system. The solvent used was 0.01 M PBS.

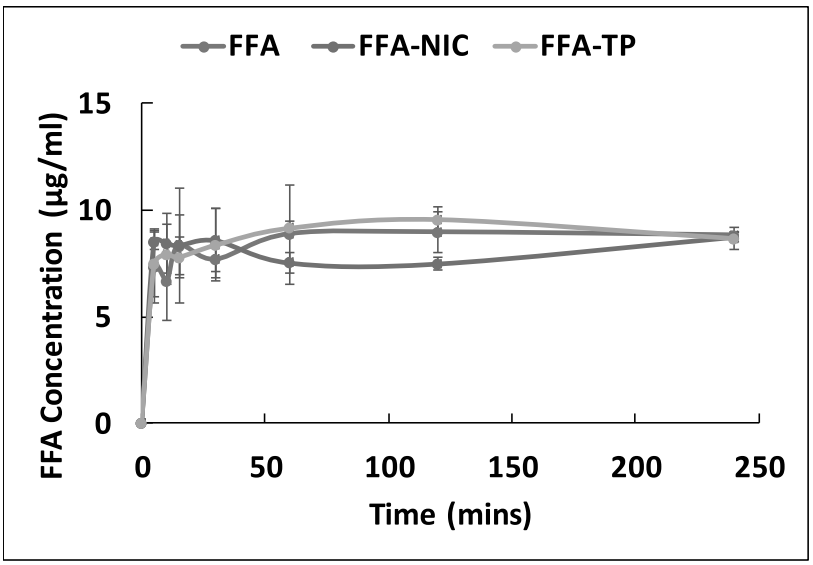

(a)

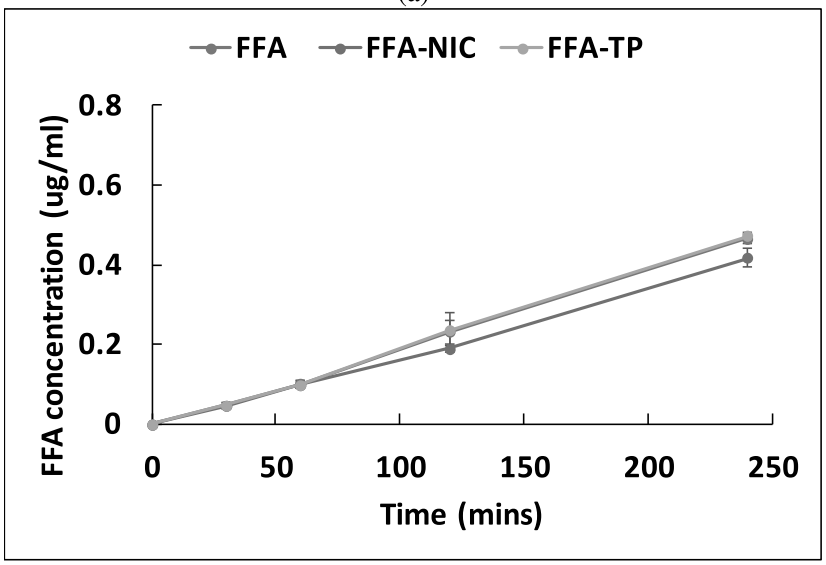

(b)

Figure 4. The D/P system was used for the DPP and flux rate measurement for FFA, FFA-NIC and FFA-TP. The donor compartment was filled with 0.01 M PBS (pH 4.5) containing either PVP or PVP-VA at concentrations of 200 μg/mL, 4000 μg/mL or 16000 μg/mL, and the receptor compartment was filled with 0.01 M PBS (pH 4.5).

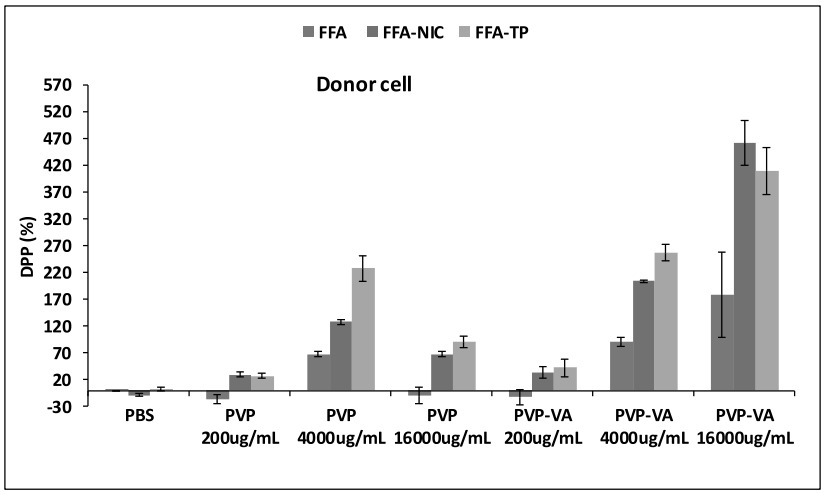

(a)

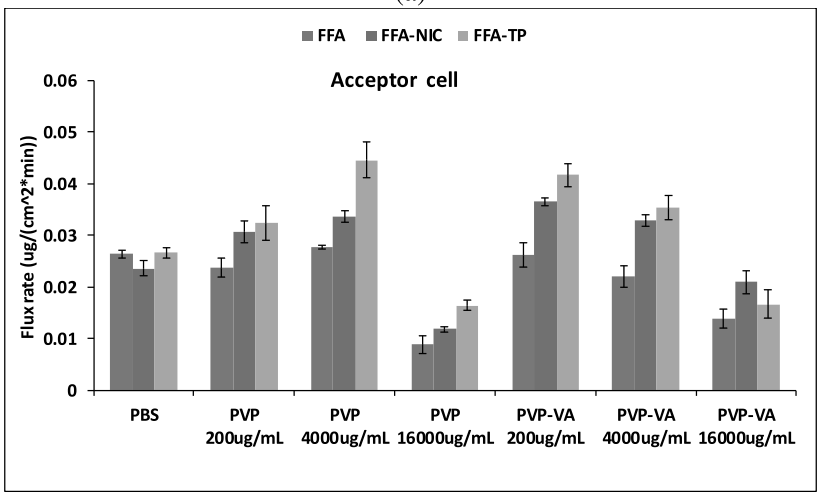

(b)

Figure 5. The dissolution and permeation of FFA, FFA-NIC and FFA-TP were investigated using the D/P system. The donor compartment was filled with 0.01 M PBS (pH 4.5) containing PVP at concentrations of 200 μg/mL, 4000 μg/mL or 16000 μg/mL, and the receptor compartment was filled with 0.01 M PBS (pH 4.5).

Pre-dissolved PVP concentration	Dissolution profile	Permeation profile
200 μg/mL	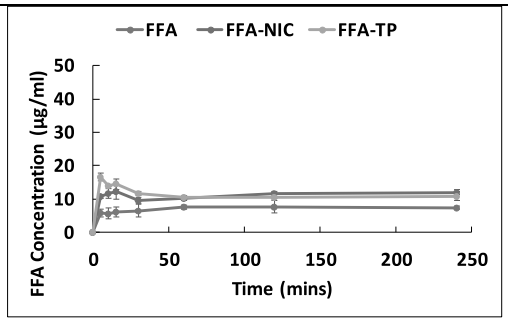 (a1)	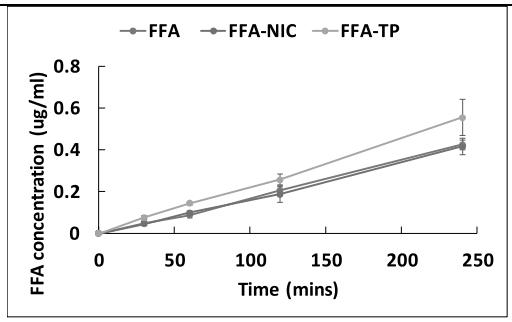 (b1)
4000 μg/mL	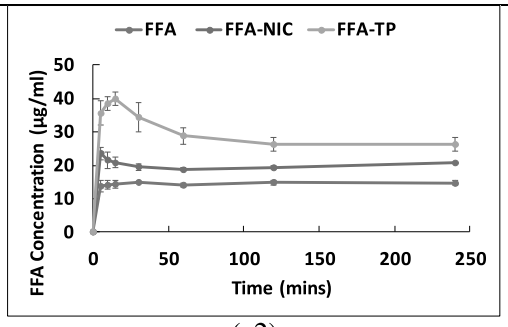 (a2)	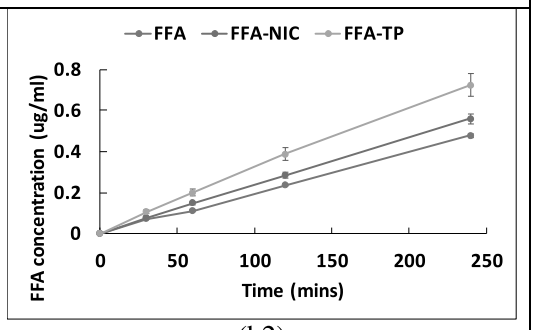 (b2)
16000 μg/mL	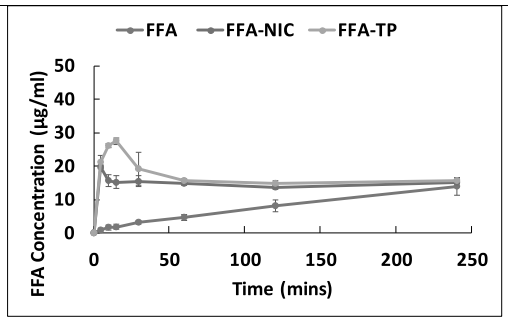 (a3)	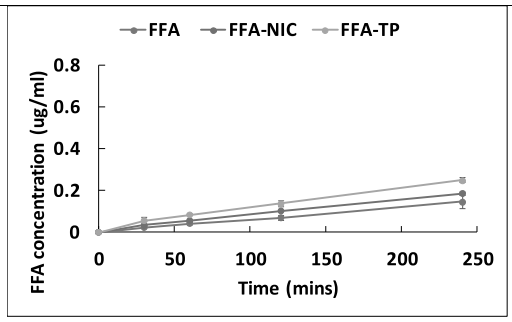 (b3)

Figure 6. The dissolution and permeation of FFA, FFA-NIC and FFA-TP were investigated using the D/P system. The donor compartment was filled with 0.01 M PBS (pH 4.5) containing PVP-VA at concentrations of 200 μg/mL, 4000 μg/mL or 16000 μg/mL, and the receptor compartment was filled with 0.01 M PBS (pH 4.5).

Pre-dissolved PVP-VA concentration	Dissolution profile	Permeation profile
200 μg/mL	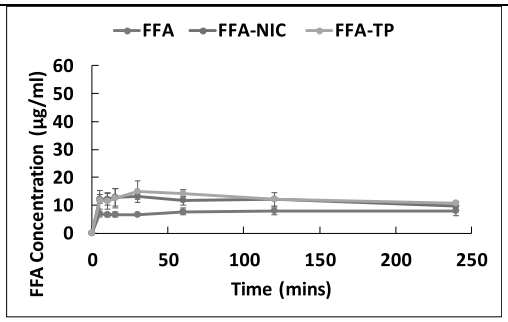 (a1)	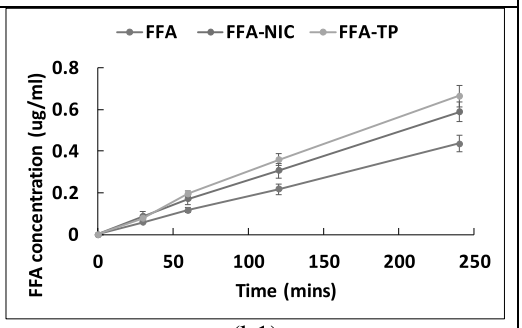 (b1)
4000 μg/mL	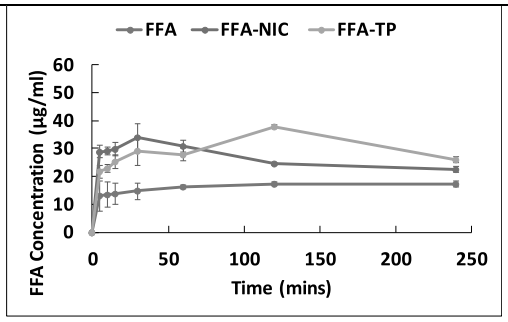 (a2)	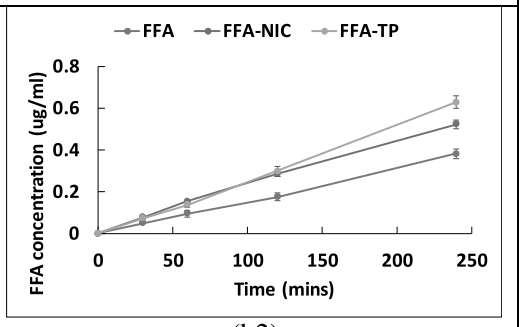 (b2)
16000 μg/mL	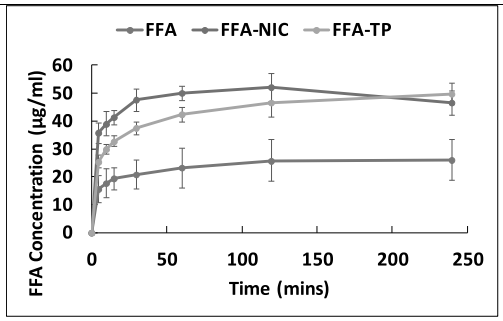 (a3)	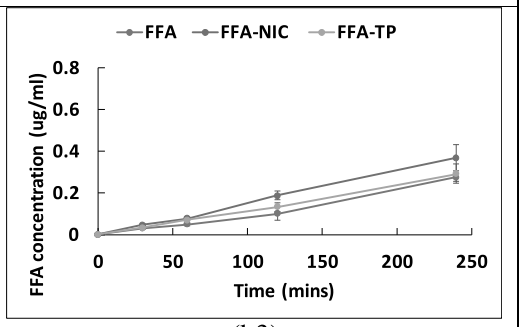 (b3)

Figure 4. 1H NMR spectra of FFA, NIC and TP. Samples of FFA (500 μg/mL, 1000 μg/mL and 5000 μg/mL), NIC (215 μg/mL, 430 μg/mL and 2150 μg/mL) and TP (320 μg/mL, 640 μg/mL and 3200 μg/mL) were prepared in deuterated chloroform ($CDCl_3$) using the standard 5 mm NMR tubes and the spectrum of tetramethysilane (TMS) was used as an internal standard.

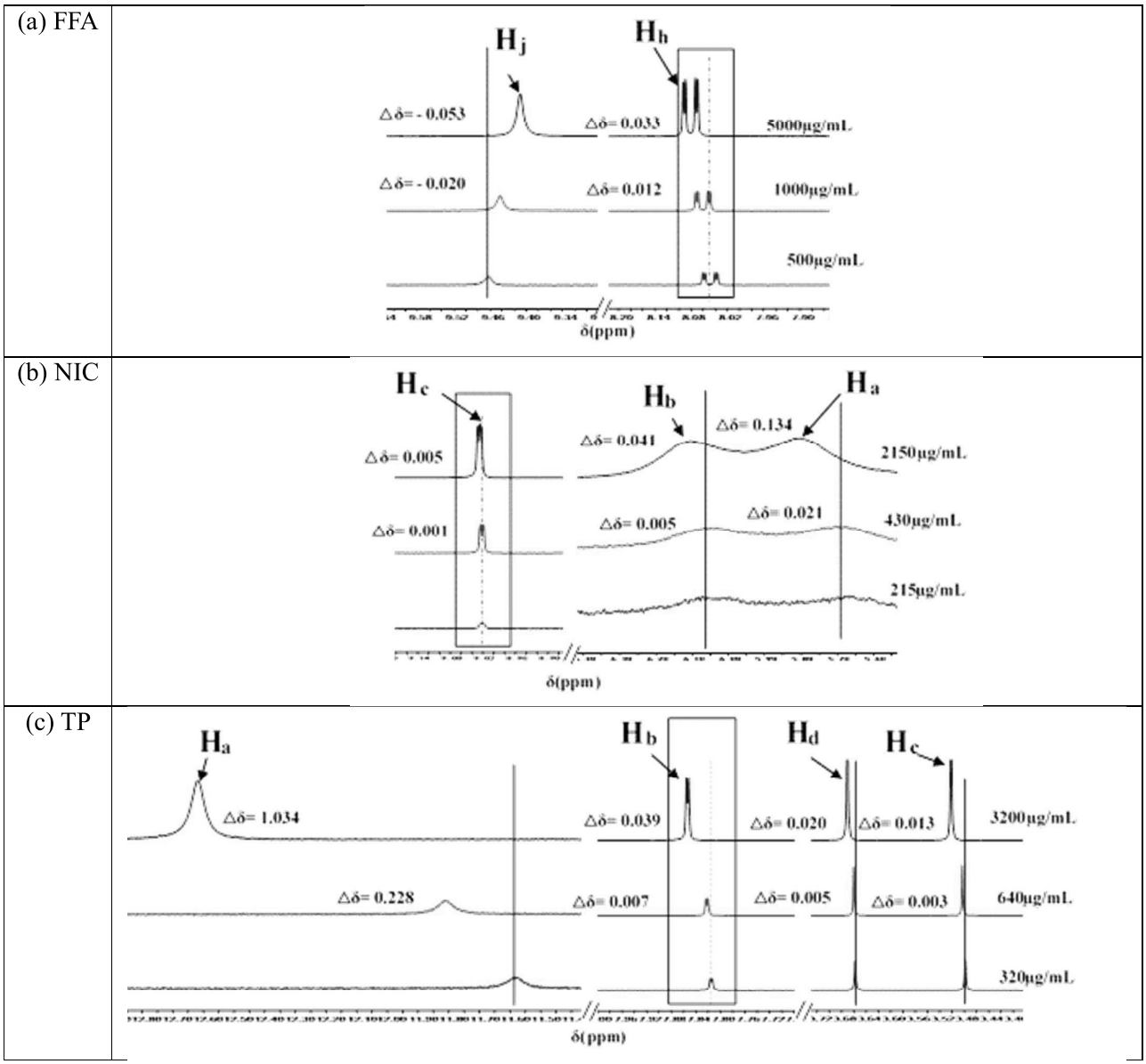

Figure 5. Effect of PVP or PVP-VA on the 1H NMR spectra of FFA, NIC and TP. Samples of FFA (1000 μg/mL), NIC (430 μg/mL) and TP (640 μg/mL) were prepared in deuterated chloroform ($CDCl_3$) using the standard 5 mm NMR tubes and the spectrum of tetramethysilane (TMS) was used as an internal standard. PVP or PVP-VA was included in the solution of $CDCl_3$ at a concentration of 200 μg/mL or 5000 μg/mL.

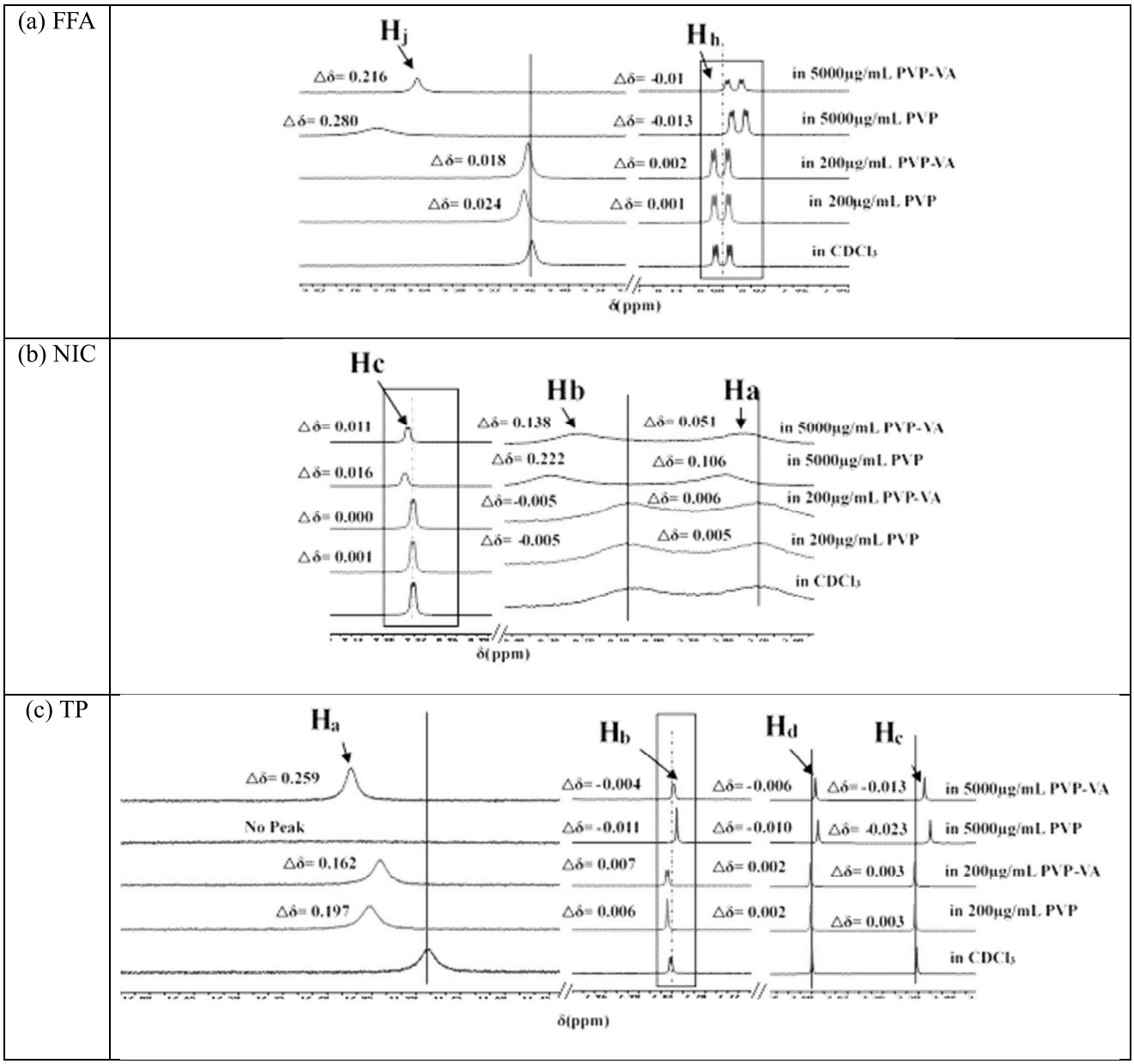

Figure 6. ^{1}H NMR spectra of mixture FFA with NIC or TP. Samples were prepared in deuterated chloroform ($CDCl_3$) using the standard 5 mm NMR tubes and the spectrum of tetramethysilane (TMS) was used as an internal standard. The FFA and its coformers were included in the $CDCl_3$ solution at 1:1 molar ratio. The concentration of FFA, NIC and TP were 1000 μg/mL, 430 μg/mL, and 640 μg/mL.

(a) 1:1 molar ratio of FFA and NIC	FFA	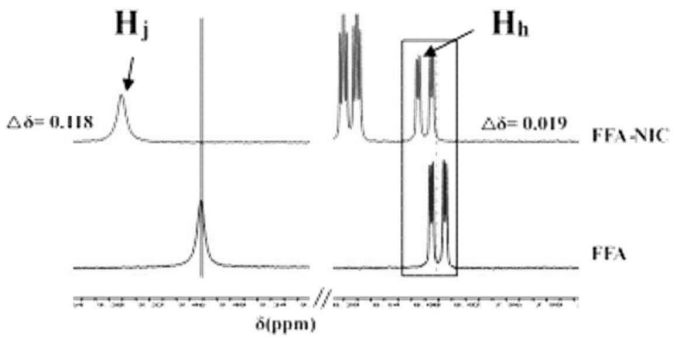
	NIC	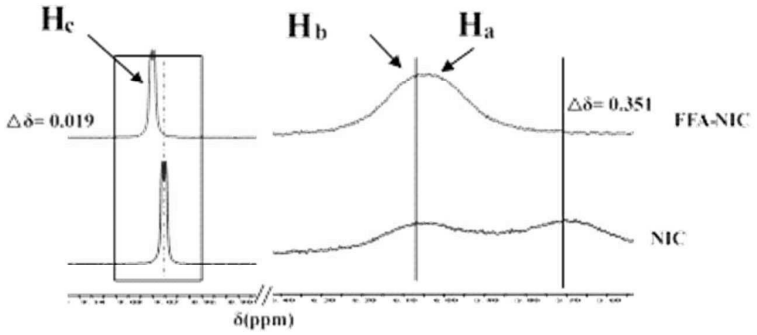
(b) 1:1 molar ratio of FFA and TP	FFA	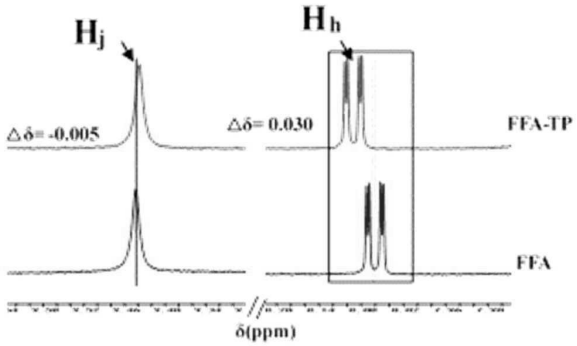

	TP	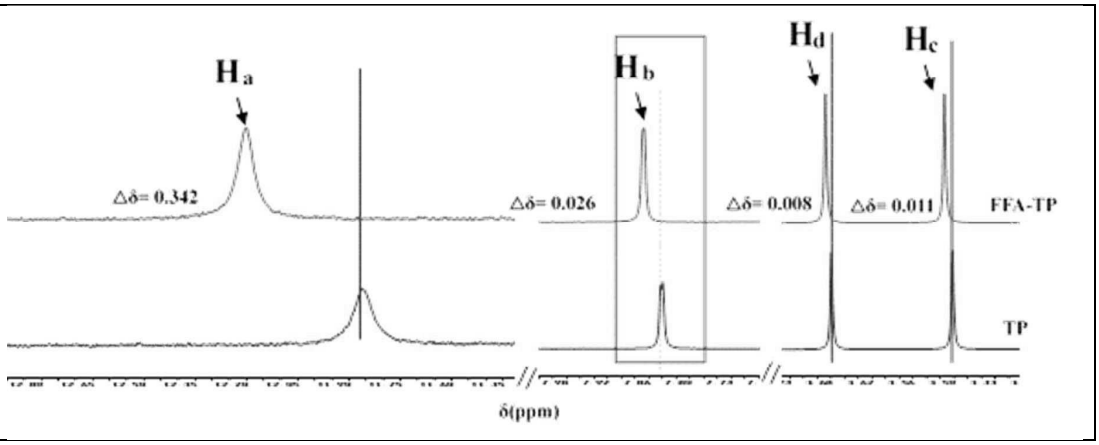 Ha Hb Hd Hc △δ= 0.342 △δ= 0.026 △δ= 0.008 △δ= 0.011 FFA-TP TP δ(ppm)

Figure 7. Effect of PVP or PVP-VA on the ^{1}H NMR spectra of mixed FFA with NIC or TP.^{1}H NMR spectra of FFA in an equal molar mixture of FFA and NIC or TP at difference concentrations of a polymer in $CDCl_3$. Samples were prepared in deuterated chloroform ($CDCl_3$) using the standard 5 mm NMR tubes and the spectrum of tetramethysilane (TMS) was used as an internal standard. The FFA and its coformers were included in the $CDCl_3$ solution at 1:1 molar ratio to obtain the concentrations of 430 μg/mL of NIC, 640 μg/mL of TP and 1000 μg/mL of FFA. PVP or PVP-VA was included in the solution of $CDCl_3$ at a concentration of 200 μg/mL or 5000 μg/mL.

1:1 molar ratio of FFA and NIC	(a) PVP	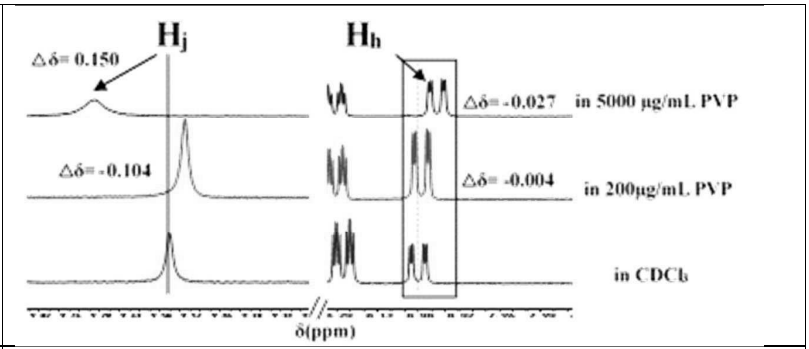
	(b) PVP-VA	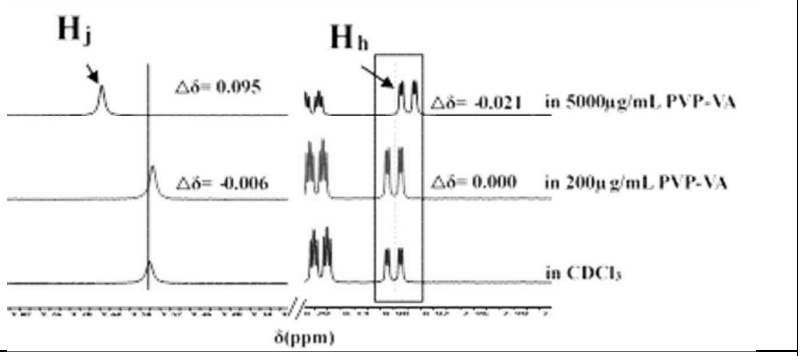
1:1 molar ratio of FFA and TP	(c) PVP	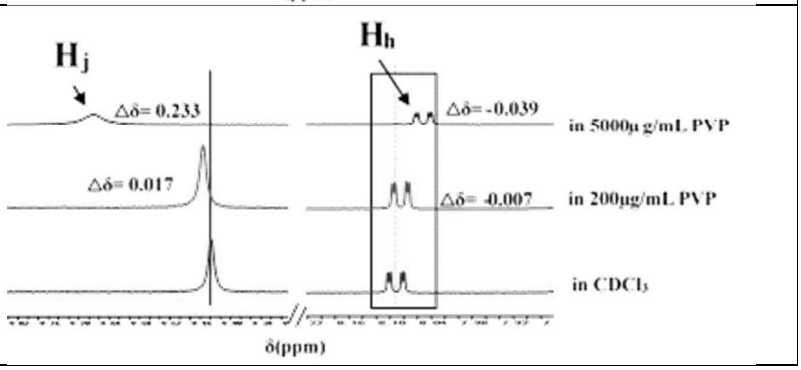

	(d) PVP-VA	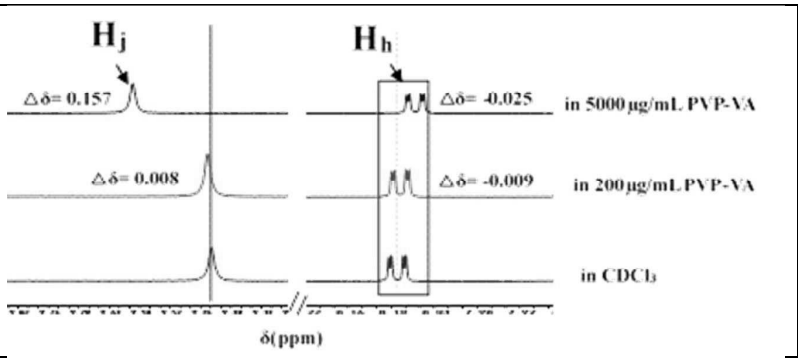 H_j H_h △δ= 0.157 △δ= -0.025 in 5000 μg/mL PVP-VA △δ= 0.008 △δ= -0.009 in 200 μg/mL PVP-VA in $CDCl_3$ δ(ppm)